NASA TECHNICAL NOTE

INVESTIGATION OF AN OPTIMUM DETECTION SCHEME FOR A STAR-FIELD MAPPING SYSTEM

by Melvin D. Aldridge and Leonard Credeur

Langley Research Center
Hampton, Va. 23365

NATIONAL AERONAUTICS AND SPACE ADMINISTRATION • WASHINGTON, D. C. • SEPTEMBER 1970

1. Report No. NASA TN D-5972	2. Government Accession No.	3. Recipient's Catalog No.
4. Title and Subtitle INVESTIGATION OF AN OPTIMUM DETECTION SCHEME FOR A STAR-FIELD MAPPING SYSTEM		5. Report Date September 1970 6. Performing Organization Code
7. Author(s) Melvin D. Aldridge and Leonard Credeur		8. Performing Organization Report No. L-6477
9. Performing Organization Name and Address NASA Langley Research Center Hampton, Va. 23365		10. Work Unit No. 125-21-04-01 11. Contract or Grant No.
12. Sponsoring Agency Name and Address National Aeronautics and Space Administration Washington, D.C. 20546		13. Type of Report and Period Covered Technical Note 14. Sponsoring Agency Code

15. Supplementary Notes Some of the material presented herein formed part of a thesis entitled "Investigation of the Optimum Detection System for a Star Field Mapping System," offered by Melvin D. Aldridge in partial fulfillment of the requirements for the degree of Master of Electrical Engineering, University of Virginia, Charlottesville, Virginia, August 1965.

16. Abstract

An investigation was made to determine the optimum detection scheme for a star-field mapping system that uses coded detection resulting from starlight shining through specially arranged multiple slits of a reticle. The computer solution of equations derived from a theoretical model showed that the greatest probability of detection for a given star and background intensity occurred with the use of a single transparent slit. However, use of multiple slits improved the system's ability to reject the detection of undesirable lower intensity stars, but only by decreasing the probability of detection for lower intensity stars to be mapped. Also, it was found that the coding arrangement affected the root-mean-square star-position error and that detection is possible with error in the system's detected spin rate, though at a reduced probability.

17. Key Words (Suggested by Author(s)) Coded light-detection system Position determination	18. Distribution Statement Unclassified – Unlimited		
19. Security Classif. (of this report) Unclassified	20. Security Classif. (of this page) Unclassified	21. No. of Pages 32	22. Price* $3.00

*For sale by the Clearinghouse for Federal Scientific and Technical Information
Springfield, Virginia 22151

INVESTIGATION OF AN OPTIMUM DETECTION SCHEME FOR A STAR-FIELD MAPPING SYSTEM*

By Melvin D. Aldridge and Leonard Credeur
Langley Research Center

SUMMARY

An investigation was made to determine the optimum detection scheme for a star-field mapping system that uses coded detection resulting from starlight shining through specially arranged multiple slits of a reticle. With threshold levels established by the Neyman-Pearson criterion, the computer solutions of equations derived from a theoretical model are used to judge performance, and then practical problems such as synchronization, code construction, and detector noise are considered.

On the basis of the Neyman-Pearson criterion it was determined that the maximum probability of detection occurred with the use of a single transparent slit in the modulating reticle. However, use of multiple slits improved the system's ability to reject the detection of undesirable lower intensity stars, but only by decreasing the detection probability of the lower intensity stars to be mapped. Also, it was found that the coding arrangement affected the root-mean-square star-position error and that detection is possible with error in the system's detected spin rate, though at a reduced probability.

INTRODUCTION

The problem investigated herein was encountered at the Langley Research Center during the design of a star-field mapping system for a spinning rocket probe (ref. 1). The system uses a coded detection scheme resulting from starlight shining through specially arranged multiple slits of a reticle. It appears desirable to use a number of slits so that more than one pulse per star will be available for a cross-correlation detection process with the known slit pattern.

The purpose of this study is to determine the optimum number and arrangement of slits (i.e., optimum codes) for maximum probability of detecting stars in the star scanner.

*Some of the material presented herein formed part of a thesis entitled "Investigation of the Optimum Detection System for a Star Field Mapping System," offered by Melvin D. Aldridge in partial fulfillment of the requirements for the degree of Master of Electrical Engineering, University of Virginia, Charlottesville, Virginia, August 1965.

In addition, the ability of the system to reject the detection of undesirable lower intensity stars is considered. Performance information is obtained by utilizing computer solutions of equations derived from a theoretical model and then considering practical problems such as synchronization, code construction, and detector noise.

Although star mapping provided the prime motivation for this study, the results can in general be applied to a light-source detection system of the type considered.

SYMBOLS

a_j	decision that x_j is true state of affairs
$1 + B$	secondary emission noise factor
b	additional noise factor
C_f	cost of falsely detecting a star
C_{ij}	cost of deciding that j occurred when i really occurred
C_m	cost of missing a star
$\overline{D}$	equivalent dark current rate, photoelectrons per sample
e	electron charge, coulombs
f_r	code repetition bit rate
$\overline{G}$	average photomultiplier gain
$\overline{I}_D$	average photomultiplier anode dark current, amperes
i,j	events
k	average number of photoelectrons emitted per second
k_n	average noise photoelectron rate per reticle slit
l	number of times 1 is detected as 1

m	number of times 0 is detected as 1
N	number of transparent slits in modulating reticle
n	number of photoelectrons
P_D	probability of detecting a star, assuming code is fully in correlator
$P_{D,1}$,$P_{D,2}$	P_D for cross-correlation detection methods 1 and 2, respectively
$P_{D,\delta}$	probability of detection for code in correlation position δ
P_{FA}	probability of false alarm
$P_{FA,1}$,$P_{FA,2}$	P_{FA} for cross-correlation detection methods 1 and 2, respectively
$P_{FA,G}$	given (allowable) P_{FA}
$P(g,N)$	probability that g events will occur out of N possible events
$P(i)$	probability that event i will occur
$P(i/j)$	probability that event i will occur, knowing that event j has occurred
P_{ij}	probability that i is detected as j (i,j either 0 or 1)
$P(n)$	probability that n photoelectrons will be emitted during time τ
P_p	probability that star is present for detection
q	number of times 0 is detected as 0
R	overall average risk of decision scheme
r_0	average cost of error when star is not present
r_1	average cost of error when star is present
s	integral multiple of exact code repetition rate

T_B	bit decision threshold
T_C	correlation decision threshold
$T_{C,1}, T_{C,2}$	T_C for cross-correlation detection methods 1 and 2, respectively
t	time
Δt	uncertainty in sample time
t_B	star pulse width in time (bit time)
t_o	beginning of detection code
t_s	sample length in time, t_B/s
x_i	condition i is true state of affairs (i either 0 or 1)
y	result of an observation
α	variable of integration of standard Gaussian distribution
Γ	signal-to-noise ratio per reticle slit (ratio of average number of star photoelectrons to average noise photoelectrons emitted per second)
$\overline{\gamma}$	average gain per dynode
δ	offset of detected code in correlator
ϵ	rms position error of star
λ	average noise photoelectrons per sample per slit
ν	error factor of sampling repetition rate
σ_T^2	total variance of theoretical statistics
τ	integration or counting time, seconds
ω	vehicle spin rate, radians/second

Subscripts:

max maximum

min minimum

GENERAL DESCRIPTION OF SYSTEM

The star-field mapping system for a spin-stabilized rocket probe which is considered in this report can be represented by figure 1. Light from the star to be detected is concentrated on the cathode of a photomultiplier tube by a telescope that has a field of view directed out of the side of the probe and is normal to the spin axis. As the vehicle rotates about its spin axis, this field of view sweeps a band in the celestial sphere. An opaque reticle with transparent slits parallel to the spin axis is positioned in the focal plane of the optics. The spin of the probe causes star images to sweep across the transparent slits, resulting in intermittent exposure of the photocathode to the images.

Thus, a train of coded current pulses appears at the tube's anode with average amplitude determined by the star's magnitude and format determined by the arrangement of the transparent slits. The form of these pulses after ideal detection is illustrated in figure 2. This coded pulse train will consist of two basic states: a 1 state occurs if a star is shining through any one of the slits, while a 0 state occurs if a star is not shining through a slit. If the coded pulse train is interpreted as a binary code, the 1's and 0's are binary digits which are commonly called bits.

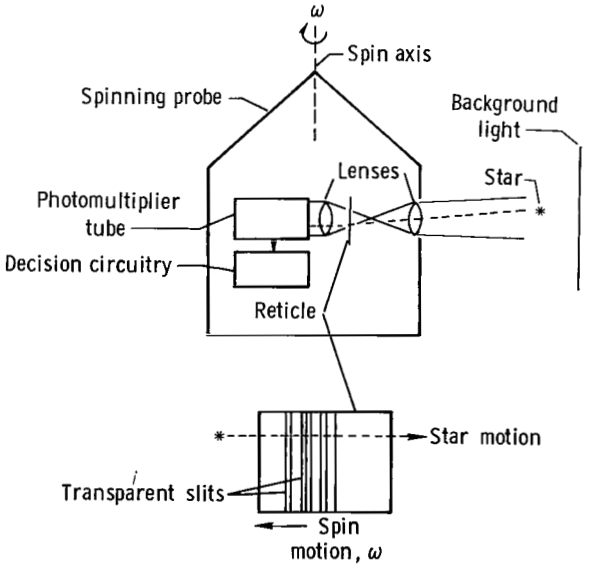

Figure 1.- Basic star-mapping system.

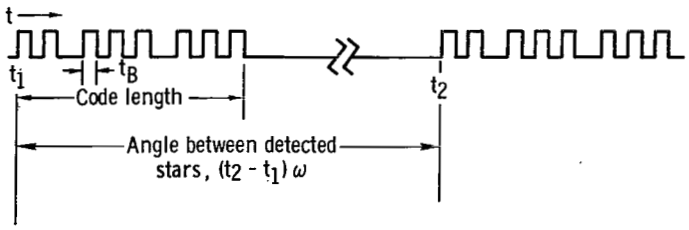

Figure 2.- Ideal bit-detection output signal.

The 0 state before detection will have an average level determined by the background light from other stars and celestial bodies in the field of view. Thus, the 1 state before detection will have an average amplitude determined not only by the star magnitude, but also by the aforementioned background light. This background light is considered as noise since it hinders the detection of the star. Also contained in the pulse train before detection will be noise generated within the photomultiplier tube and photon noise due to the quantum nature of light.

In reality, background light consists of discrete stars distributed over a wide range of magnitudes; however, it is convenient to consider that the aggregate of the very dim stars and celestial bodies constitutes a spatially homogeneous background light. Consequently, stars of sufficient brightness to allow reasonable detection probability can be considered as point light sources on top of the background. In the practical system it is desirable to map only stars whose intensity is sufficient to allow reliable detection, while rejecting (not detecting) all stars of less intensity. This will be referred to as the rejection property of a detection scheme.

SIMPLIFIED THEORETICAL ANALYSIS

Because of the many dependent variables involved, it is expedient to conduct the theoretical analysis on a simplified basis. This section first presents such a simplification and the associated assumptions. After development of the equations necessary to describe the entire detection process, the results of computer solutions are presented.

Simplification and Assumptions

The system can be represented by the simplified block diagram in figure 3. Since the photomultiplier tube is a photon- or quantum-sensitive device, the basic detection process can be simplified by counting the discrete photoelectrons (see appendix for justification). As shown in the block diagram, two separate decision processes take place in the overall detection system. First is the bit detection, which attempts to determine if a star is or is not shining through a slit. Second is the cross-correlation detection, which

determines whether an adequate number (with the proper arrangement or coding) of these bits have been detected to ascertain the presence of a star. We can suppose that the correlator consists of a shift register into which the results of the bit detection are serially fed. The contents of the register are compared at each bit time with the known code determined by the reticle slit configuration. This comparison is the basis of the cross-correlation detection process.

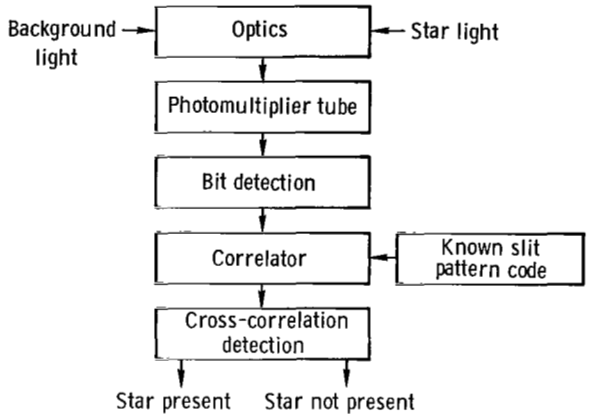

Figure 3.- System block diagram.

The following assumptions will be made for the simplified theoretical analysis:

1. The bit detector counts discrete photoelectrons.

2. Samples are taken only when the star image lies wholly within or not within a slit (i.e., bit synchronization is known).

3. Either a complete code due to the presence of a star or only detected noise bits exist in the correlator. That is, the correlation that takes place while serially shifting the code bits (due to the presence of a star) into and out of the correlator will be neglected for now.

4. Noise generated within the photomultiplier will be ignored.

5. The effect of having two stars of sufficient intensity for reliable detection within the field of view simultaneously will be neglected.

6. The average number of emitted photoelectrons per sampling period will be large enough to allow the Poisson distribution to be approximated by the normal distribution (ref. 2).

7. The number of 1's and the number of 0's for a given coding arrangement are taken to be equal. Also, the pulse widths (bit times) of the 1's and 0's are assumed to be equal.

In addition, it is assumed that the resolution of the optics is much better than the width of a transparent slit. Thus the resulting pulse will have nearly instantaneous rise and decay times. Otherwise the problem involves time-variable statistics, which is beyond the scope of this paper. The effects on a practical system when assumptions 2, 3, and 4 are not made will be considered later in the paper.

Bit-Detection Analysis

Bit detection involves the counting of discrete photoelectrons which are emitted from the photocathode during the sample period. These emitted electrons will possess conventional shot noise and thus will have a Poisson statistical distribution (ref. 3). This distribution is expressed by the relation

$$P(n) = \frac{(k\tau)^n}{n!} \exp(-k\tau) \tag{1}$$

where

n number of photoelectrons

k average number of photoelectrons emitted per second

τ counting or integration time, seconds

$P(n)$ probability that n photoelectrons will be emitted during time τ

The statistics can be completely described from a knowledge of the average signal and noise photoelectron rates and the integration time τ. These rates are defined by

k_n average noise photoelectron rate per reticle slit

Γ signal-to-noise ratio per reticle slit (ratio of average number of star photoelectrons to average noise photoelectrons emitted per second)

If the background light is considered as having homogeneous spatial density over the entire celestial sphere, the total background noise falling on the photocathode becomes a linear function of the number of slits in the reticle. Since synchronization information is known by assumption 2, τ can be made equal to t_B, where t_B is the star pulse width in time (bit time). The total average number of photoelectrons emitted per sample period is

$$\text{Signal + Noise} = k_n t_B(N + \Gamma) = \lambda(N + \Gamma) \tag{2}$$

where

N total number of transparent slits

λ average noise photoelectrons per sample per slit, $k_n t_B$

These relations can now be applied to the Poisson distribution to describe the bit detection statistics. A bit threshold T_B establishes the decision level. If the count during an integration period falls below this level, the decision is made that a 0 was present, or that no star was shining through a slit. Similarly, if the count appears at T_B or above, the decision is made that a 1 was present, or a star was shining through one of the slits. The probability that a 0 will be detected as a 0 is

$$P_{00} = \sum_{n=0}^{T_B-1} \frac{(N\lambda)^n}{n!} \exp(-N\lambda) \tag{3}$$

and the probability that a 1 will be detected as a 1 is

$$P_{11} = \sum_{n=T_B}^{\infty} \frac{\left[\lambda(N + \Gamma)\right]^n}{n!} \exp\left[-\lambda(N + \Gamma)\right] \tag{4}$$

As discussed by Feller (ref. 2), the Poisson distribution can be approximated with good accuracy by a Gaussian distribution whenever the average value $N\lambda$ is sufficiently large, as stated in assumption 6. Thus, in the rest of this paper equations (3) and (4) will be approximated by

$$P_{00} = \frac{1}{\Pi} \int_{-\infty}^{\frac{T_B-N\lambda}{\sqrt{2N\lambda}}} \exp(-\alpha^2)d\alpha \tag{5}$$

$$P_{11} = \frac{1}{\Pi} \int_{\frac{T_B-\lambda(N+\Gamma)}{\sqrt{2\lambda(N+\Gamma)}}}^{\infty} \exp(-\alpha^2)d\alpha \tag{6}$$

As will be found later, these Gaussian forms are convenient for the inclusion of photomultiplier noise in the analysis. These relations express the probabilities of correct bit

decision. The probabilities of false bit decision are then

$$P_{01} = 1 - P_{00} \tag{7}$$

$$P_{10} = 1 - P_{11} \tag{8}$$

where

P_{01} probability a 0 is detected as a 1

P_{10} probability a 1 is detected as a 0

It should be noted that for the special case of only one slit, the bit detection and correlation detection are synonymous, and equations (3) to (8) completely describe the system. For this case the probability of detecting a star when it is present is P_{11} and the probability of a false alarm is P_{01}.

Cross-Correlation Detection Analysis

As a result of the bit-detection process, the coded signal for each star consists of a series of 1's and 0's whose signal format is referred to as PCM (pulse-code-modulated) nonreturn-to-zero format. Cross-correlation between the detected bit code and a known code, determined by the geometric pattern of the transparent slits in the reticle, forms the basis for the cross-correlation detection. Knowing the detection criterion, it is possible to calculate the probability of detecting a star if it is assumed that all the code bits from the presence of a star have been shifted into the proper correlation position (see assumption 3). Similarly, the probability of false alarm can be calculated by assuming that the detected bit code in the correlator should consist of all 0 bits in the absence of a star. For analysis, two different cross-correlation schemes will be utilized. Many schemes are possible, allowing different weights to the proper detection of 0's. The two methods chosen are extremes of a sort: (1) No weight placed on proper 0 detection; (2) equal weight placed on proper 0 and 1 detection.

Method 1 – "one" detection only.- The first technique is concerned only with the 1 bits and does not consider the 0's that occur as a result of the opaque area between slits of the modulating reticle. A correlation threshold $T_{C,1}$ can be defined so that $T_{C,1}$ or more 1 bits must agree with the 1 bits of the known code for the presence of the star to be detected. The binominal statistical distribution applies, since there exist N possible events, each with the same probability of occurrence. This distribution is described by the relation (ref. 4)

$$P(g,N) = \frac{N!}{g!(N - g)!} P(i)^{g}\left[1 - P(i)\right]^{N-g} \tag{9}$$

where

N total number of possible times event i can occur (number of slits)

P(i) probability that event i will occur

P(g,N) probability that event i will occur g times out of N possible times

Thus the overall probabilities of star detection and false alarm for method 1 are expressed as

$$P_{D,1} = \sum_{l=T_{C,1}}^{N} \frac{N!}{l!(N - l)!} P_{11}{}^{l}\left(1 - P_{11}\right)^{N-l} \tag{10}$$

$$P_{FA,1} = \sum_{m=T_{C,1}}^{N} \frac{N!}{m!(N - m)!} P_{01}{}^{m}\left(1 - P_{01}\right)^{N-m} \tag{11}$$

Method 2 – "zero-one" detection.- The second technique treats the proper detection of 0's and 1's as being equally important. At this point it should be recalled that in assumption 7 both the pulse width and the number of the 0's are equal to those of the 1's. A threshold $T_{C,2}$ can be defined so that the total sum of all properly detected 1's and 0's must be equal to or greater than $T_{C,2}$ for the presence of a star to be determined. The value of $T_{C,2}$ shall be greater than N. Although the statistics again follow from equation (9), all possible combinations of 0's and 1's that will give $T_{C,2}$ or greater must be included. Assuming that the 0's and 1's are independent, the probability of star detection for method 2 becomes

$$P_{D,2} = P\left(1\text{'s} + 0\text{'s} \geq T_{C,2}\right) = \sum_{l=T_{C,2}-N}^{N}\left[\sum_{q=T_{C,2}-l}^{N} P_{00}(q,N)\, P_{11}(l,N)\right] \tag{12}$$

where

$$P_{00}(q,N) = \frac{N!}{q!(N - q)!} P_{00}{}^{q}\left(1 - P_{00}\right)^{N-q}$$

$$P_{11}(\ell,N) = \frac{N!}{\ell!(N-\ell)!} P_{11}{}^{\ell}\left(1 - P_{11}\right)^{N-\ell}$$

Similarly, for the probability of false alarm,

$$P_{FA,2} = \sum_{m=T_{C,2}-N}^{N}\left[\sum_{q=T_{C,2}-m}^{N} P_{00}(q,N)\, P_{01}(m,N)\right] \tag{13}$$

where

$$P_{01}(m,N) = \frac{N!}{m!(N-m)!} P_{01}{}^{m}\left(1 - P_{01}\right)^{N-m}$$

Choice of Thresholds

Although bit and correlation thresholds were defined in the preceding sections, their magnitudes were not discussed. Their proper choice depends directly on the establishment of an optimum system criterion. One such criterion exists in Bayes' decision rule, which defines the conditions that minimize the overall cost of detection errors (ref. 5). Threshold magnitudes will now be considered by applying Bayes' decision rule.

Let the true state of affairs be represented by x_0 when a star is not present and by x_1 when a star is present. Let y represent the results of an observation related to the true state of affairs; it can be related to the true state of affairs by two probability density functions in the following matrix form:

$$\begin{array}{c} \\ x_0 \\ x_1 \end{array}\begin{array}{c} y \\ \left[\begin{array}{c} P(y/x_0) \\ P(y/x_1) \end{array}\right] \end{array} \tag{14}$$

If a_j represents the decision that x_j is the true state of affairs when x_i is really the true state, the relationship can be represented by

$$\begin{array}{c} \\ x_0 \\ x_1 \end{array}\begin{array}{c} a_0 \qquad\qquad a_1 \\ \left[\begin{array}{cc} P(a_0/x_0) & P(a_1/x_0) \\ P(a_0/x_1) & P(a_1/x_1) \end{array}\right] \end{array} \tag{15a}$$

A relative cost C_{ij} of the above decision can be assigned as

$$\begin{array}{c} \\ x_0 \\ x_1 \end{array}\begin{array}{c} \begin{array}{cc} a_0 & a_1 \end{array} \\ \begin{bmatrix} C_{00} & C_{01} \\ C_{10} & C_{11} \end{bmatrix} \end{array} = \begin{array}{c} \\ x_0 \\ x_1 \end{array}\begin{array}{c} \begin{array}{cc} a_0 & a_1 \end{array} \\ \begin{bmatrix} 0 & C_f \\ C_m & 0 \end{bmatrix} \end{array} \tag{15b}$$

where

$C_{00} = C_{11} = 0$ since no cost is associated with a true decision

$C_{01} = C_f$ cost of falsely deciding a star was present

$C_{10} = C_m$ cost of missing a star

The average cost of error when the star is present is

$$r_1 = C_m P(a_0/x_1) \tag{16}$$

The average cost of error when the star is actually not present is

$$r_0 = C_f P(a_1/x_0) \tag{17}$$

Note that

$P(x_1) = P_p$ (probability that a star is present)

$P(x_0) = 1 - P_p$

$P(a_1/x_1) = P_D$ (probability of detecting a star)

$P(a_0/x_1) = 1 - P_D$

$P(a_1/x_0) = P_{FA}$ (probability of false alarm)

$P(a_0/x_0) = 1 - P_{FA}$

The overall average risk is

$$R = P_p r_1 + (1 - P_p) r_0 = P_p C_m (1 - P_D) + (1 - P_p) C_f P_{FA} \tag{18}$$

From Bayes' decision rule, the threshold should be chosen so that R is minimized.

At this point it would be helpful to discuss the relative magnitudes of P_p, C_m, and C_f for a practical mapping system. A typical field of view might be 6^o with slits of approximately 1 minute of arc. This is only a small percentage of the total steradians scanned during a vehicle rotation. Because of the relatively low density of stars bright enough for reliable detection, only a small percentage of the total time of a vehicle's rotation is involved in a positive detection process. In other words, the system will be vulnerable to false alarms much longer than it will be involved in detecting a star. Therefore

$$\left(1 - P_p\right) >> P_p \tag{19}$$

If it is assumed that the cost of one false alarm is about the same as the cost of missing a star, C_f and C_m are of the same order of magnitude. Furthermore, it is always desirable to have

$$P_D > P_{FA} \tag{20}$$

With the above relative magnitudes in mind, it can be seen from equation (18) that if the ratio P_D/P_{FA} is maximized, the total risk R is minimized. However, the maximization of this ratio relies only on the relative rates of change of P_D and P_{FA} for a varying threshold. Since decreasing P_D also decreases P_{FA}, and vice versa, such a maximization can occur for false rates much lower (or higher) than those allowable, which could give a P_D much lower than would have been obtained if the allowable P_{FA} had been utilized. Thus, it appears convenient to establish an allowable P_{FA} and then choose thresholds to minimize $1 - P_D$ or maximize P_D. This is known as the Neyman-Pearson criterion.

Method of Computer Analysis

Equations (5), (6), and (10) to (13) were programed on a digital computer. The Neyman-Pearson criterion was used by choosing an allowable false alarm probability $P_{FA,G}$. A correlation threshold T_C was chosen, and P_{00} was determined from equation (11) or (13) by an iterative process which gave P_{FA} within 1 percent of $P_{FA,G}$ on the low side. From equation (5) the T_B which gave this P_{00} to within 0.00001 percent on the low side was determined. The probabilities P_{11} and P_D were then calculated. This procedure was followed for both methods of cross-correlation. By varying the correlation threshold T_C for given values of λ, Γ, and N, an optimum correlation threshold could be found that gave the maximum possible P_D. Then by varying N and using its corresponding optimum T_C values for given values of λ, Γ, and $P_{FA,G}$, the variation of P_D was studied. This procedure was repeated for various combinations of λ, Γ, and $P_{FA,G}$.

Discussion of Theoretical System Analysis

As indicated in the preceding section, the problem in calculating the maximum P_D for given values of λ, Γ, and N is the proper choice of a correlation threshold T_C. In figure 4, P_D is shown as a function of T_C for various values of Γ. These curves show that an optimum threshold exists. However, note that as Γ increases the curve flattens, and thus the criticalness of the optimum choice decreases. Although it is not easily shown in graphical form, as Γ increases the optimum threshold level tends to decrease. These characteristics are true also for a change of any variable which increases P_{11} (i.e., increasing P_{11} increases P_D and flattens the curve).

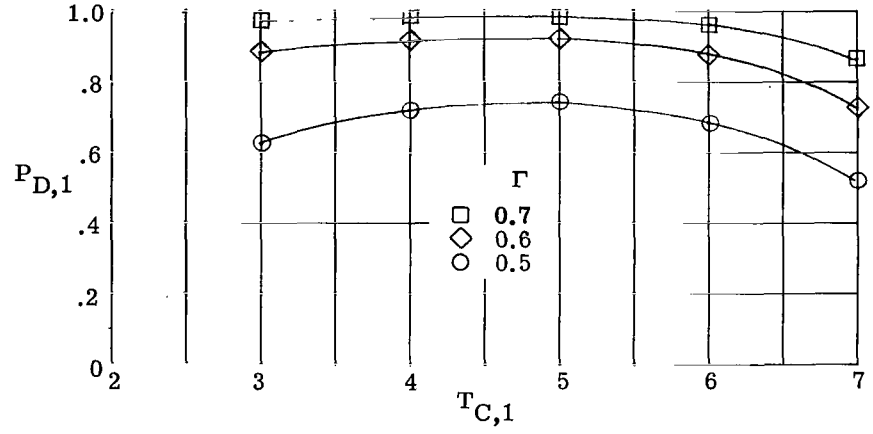

(a) Cross-correlation method 1: detection of 1's only.

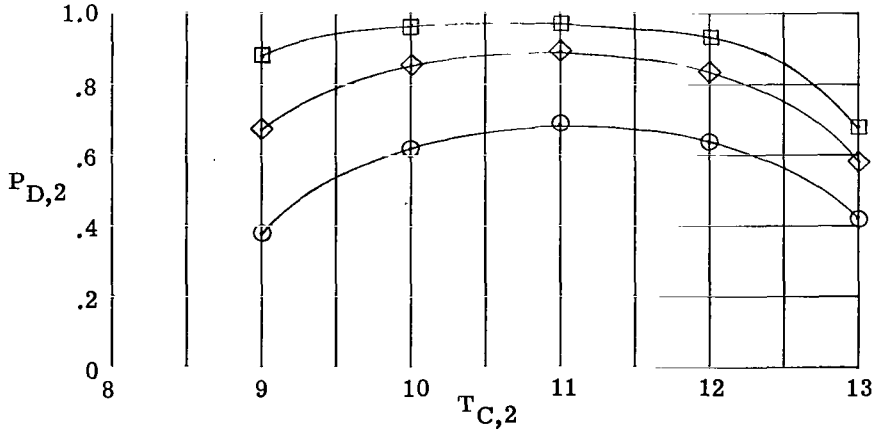

(b) Cross-correlation method 2: detection of 1's and 0's.

Figure 4.- Probability of detection as a function of correlation threshold. $N = 7$; $\lambda = 100$; $P_{FA,G} = 10^{-5}$.

The optimum number of slits for a maximization of the probability of detection will be considered next. In each of the following cases, for a given number of slits N, the corresponding optimum T_C was used.

Figure 5 shows that increasing λ increases P_D. At first thought this might appear incorrect, since an increase in λ involves increases in both background noise photoelectrons and star photoelectrons, and these are increased in the same proportion because Γ is constant. Inspection of the first and second moments of the Poisson distribution shows that the mean increases as λ, while the rms deviation increases as $\sqrt{\lambda}$.

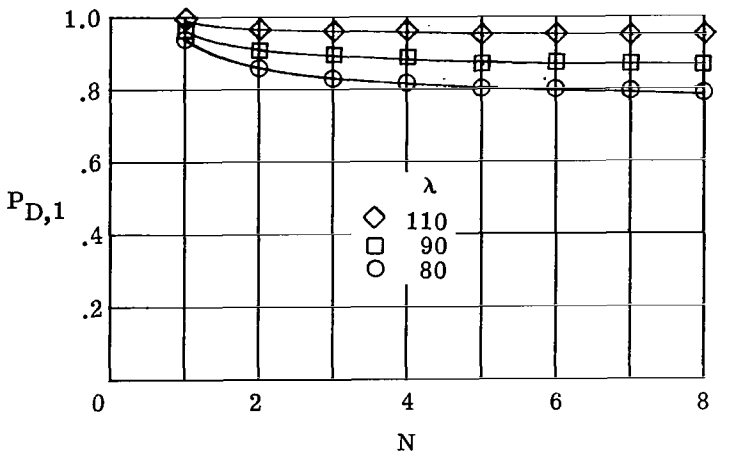

(a) Cross-correlation method 1: detection of 1's only.

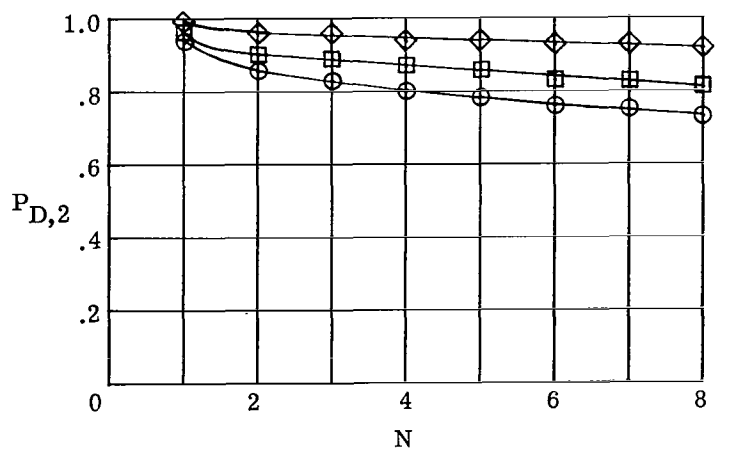

(b) Cross-correlation method 2: detection of 1's and 0's.

Figure 5.- Probability of detection as a function of number of slits and noise strength. $\Gamma = 0.7$; $P_{FA,G} = 10^{-5}$.

Thus the ability to discriminate between the noise distribution, with mean λN, and the signal-plus-noise distribution, with mean $\lambda(N + \Gamma)$, has improved although the noise level has increased.

As expected, figures 6 and 7 show that increasing Γ or P_{FA} increases P_D. As N increases, P_D decreases faster for lower Γ, and also $P_{D,2}$ appears to decrease slightly faster than $P_{D,1}$ for given values of λ, Γ, and $P_{FA,G}$. These properties are better exhibited by plotting P_D as a function of Γ, as shown in figure 8 for N = 1, 3, and 8. Since decreasing star brightness is analogous to decreasing Γ,

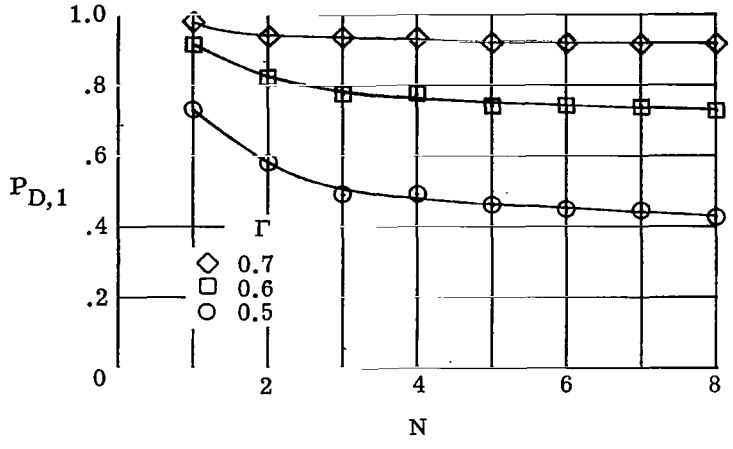

(a) Cross-correlation method 1: detection of 1's only.

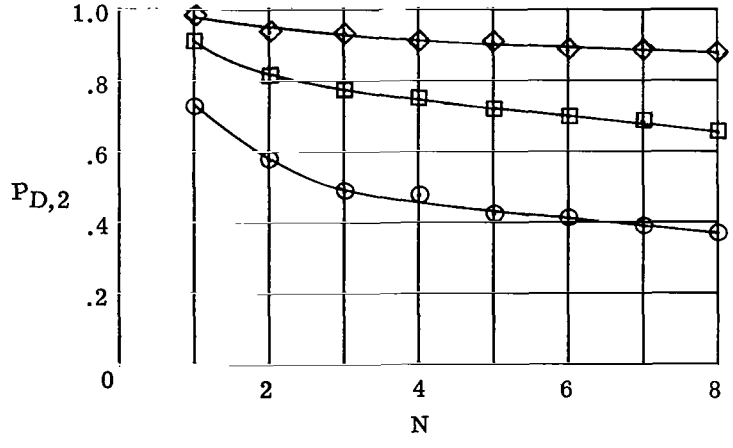

(b) Cross-correlation method 2: detection of 1's and 0's.

Figure 6.- Probability of detection as a function of number of slits and signal-to-noise ratio. $\lambda = 100$; $P_{FA,G} = 10^{-5}$.

these characteristics are the desirable ones for improving the rejection property, that is, the ability of the system to reject (not detect) stars of undesirable lesser intensity. Thus, increasing N increases the rejection property. For values of Γ of about 0.8 or higher, P_D in figure 8 is almost the same for all values of N, but for lower Γ values, P_D is considerably less for greater N.

It is interesting that the optimum correlation threshold T_C discussed earlier is used to the advantage of the code's rejection property. This is accomplished by setting T_C at the optimum value for the larger values of Γ, thus maximizing P_D for the star magnitude to be mapped. As Γ decreases, the optimum T_C increases (see discussion

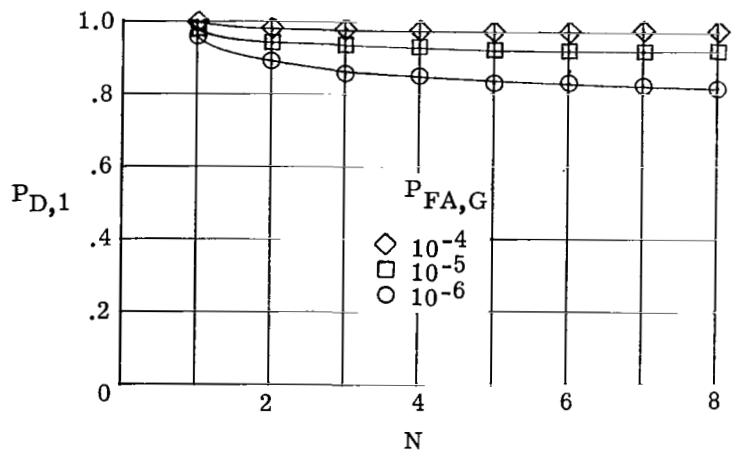

(a) Cross-correlation method 1: detection of 1's only.

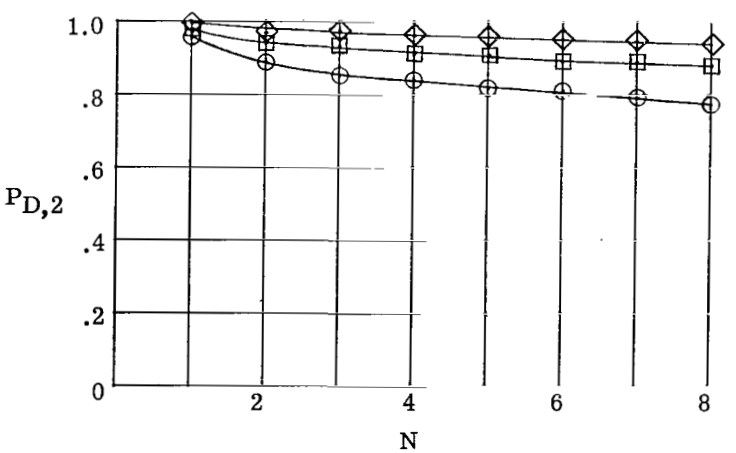

(b) Cross-correlation method 2: detection of 1's and 0's.

Figure 7.- Probability of detection as a function of number of slits and false-alarm probability. $\lambda = 100$; $\Gamma = 0.7$.

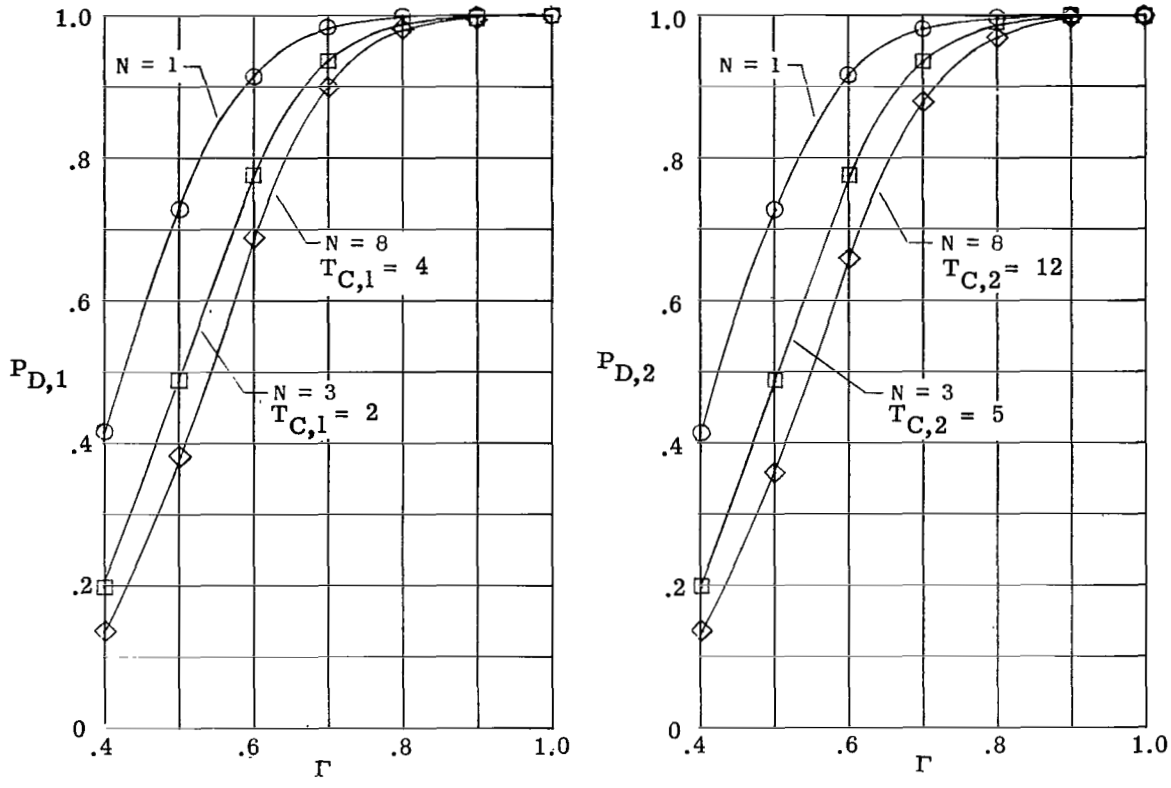

(a) Cross-correlation method 1: detection of 1's only.

(b) Cross-correlation method 2: detection of 1's and 0's.

Figure 8.- Probability of detection as a function of signal-to-noise ratio and number of slits. $\lambda = 100$; $P_{FA} = 10^{-5}$.

of fig. 4), and thus P_D decreases not only because of decreasing Γ, but also because T_C is not at its optimum value at the lower Γ.

In all cases considered, maximum P_D occurred for one slit. Thus, use of multiple slits did not improve P_D as was anticipated at the beginning of this study. Increasing the number of slits decreases the overall signal-to-noise ratio Γ/N involved in detecting 1 bits, so that P_{11} should be reduced if T_B is chosen to maintain some desired value of P_{01}. This same effect is carried over to correlation detection, and the advantage of increasing code length at fixed $P_{FA,G}$ is apparently more than offset by the degrading effect on detection of 1's.

CONSIDERATIONS FOR PRACTICAL SYSTEMS

The results of the preceding section apply only to an idealized situation which is not possible in practice. In this section the effects of code construction, synchronization limitations, and photomultiplier tube noise are studied. Equations are derived which

permit the inclusion of these parameters in the analysis of the bit and cross-correlation detection processes.

Code Construction

In the simplified theoretical analysis the probability of detection was calculated according to assumption 3. That is, either the entire code (not necessarily correct) from the presence of a star was properly placed in the correlator, or only samples of background noise were in the correlator. Thus only the code length, not the arrangement, affected the resulting statistics.

The coding arrangement does affect the probability of false alarm as the detected code of a star is shifted into and out of the correlation process. A false alarm during this process will reflect directly as an error or uncertainty in the indicated star position. Consequently, it is desirable to choose an arrangement that minimizes the rms position error. This requires that the probability of a detection be calculated for each code offset in the correlator. The code offset is defined as the number of positions in the correlator before (-) or after (+) the situation where the received code is properly placed for a direct comparison with the known code, that is, the correct star position. Calculating the probability of detection for each code offset can be a lengthy and complicated process since all possible combinations that can result in a false detection must be taken into account. The results of such a calculation from equation (9) for two codes are presented in table I.

An arbitrary code length of six bits was chosen in keeping with assumption 7. The criterion for selection of the two codes 110010 and 110100 was the minimum probability of false synchronization for a six-bit code (ref. 6). The codes are compared for

TABLE I.- ROOT-MEAN-SQUARE POSITION-ERROR CALCULATIONS FOR CODE COMPARISON

Received digit . . .	1	0	1	0	Code offset in correlator, δ		Probability of detection for various code offset positions, $P_{D,\delta}$		Root-mean-square position-error calculations			
									Code 110010		Code 110100	
Desired digit . . .	1	0	0	1	Code 110010	Code 110100	Method 1	Method 2	Method 1	Method 2	Method 1	Method 2
Number of bits in above situation	0	3	0	3	5	4, 5	0.9928×10^{-5}	0.9984×10^{-5}	24.82×10^{-5}	24.96×10^{-5}	40.70×10^{-5}	40.93×10^{-5}
	0	2	1	3	-5, 2	-5	.9928	.1260	28.79	3.65	24.82	3.15
	1	2	1	2	1, -3, -4	1, -3	292.76	36.171	7611.76	940.45	2927.60	361.71
	0	1	2	3	-2	-4	.9928	.0654	3.97	.26	15.88	1.05
	1	1	2	2	-1	-2, -1	292.76	7.2083	292.76	7.21	1463.80	36.04
	1	3	0	2	3, 4	2, 3	292.76	301.1739	7319.00	7529.35	3805.88	3915.26
	3	3	0	0	0	0	$P_{D,1}$	$P_{D,2}$	0	0	0	0
								Mean square, ϵ^2 =	15281.10×10^{-5}	8505.88×10^{-5}	8278.68×10^{-5}	4358.14×10^{-5}
								ϵ^2 =	0.1528110	0.0850588	0.0827868	0.0435814
								Root mean square, ϵ =	0.3909104	0.291649	0.287727	0.2087616

$P_{FA} \approx 10^{-5}$, $\lambda = 100$, and $\Gamma = 0.7$. From the computer program results, P_{00}, P_{11}, and T_C are known and are applied to each of the possible combinations of received and known bit patterns for detection probability. In the following example the upper code is the known code and the lower code represents a received star code preceded and followed by 0's which are represented by x's:

```
      |110010|
x|xxx|110|010xx
 ⟵
```

In this example the code offset position in the correlator is -3, and as the first four columns of table I indicate for this case, there is one agreement of 1's and two agreements of 0's; for perfect agreement, another 1 would be detected as a 0 and two more 0's would be detected as 1's. A detection would occur whenever any combination of these situations would cause T_C to be equaled or exceeded. Once $P_{D,\delta}$ was calculated for each offset, the rms position error relative to zero offset was calculated from the relation

$$\epsilon^2 = \sum_{\delta=1-2N}^{2N-1} \delta^2 P_{D,\delta} \tag{21}$$

where

δ offset of detected code in correlator

$P_{D,\delta}$ probability of detection for offset δ

ϵ rms position error relative to correct star position

Table I shows that the lowest ϵ occurs with the 110100 code and method 2 cross-correlation detection. No matter which correlation method was used, the same code was superior. Also, for either code, method 2 was superior. The reason for this can be seen in figure 9, where $P_{D,\delta}$ is shown as a function of δ for each of the situations. The dashed line indicates the level of P_{FA} when no star code elements are in the correlator. Note that for method 2, where both 0's and 1's are cross correlated, $P_{D,\delta}$ can fall below the dashed line, thus decreasing the rms position error. Because of this characteristic, errors due to shifting detected star codes into the correlator are less likely for method 2 cross-correlation detection.

Since the calculation of $P_{D,\delta}$ is rather lengthy, it is convenient to make a qualitative comparison of codes by plotting the curves shown in figure 10. Here it is assumed

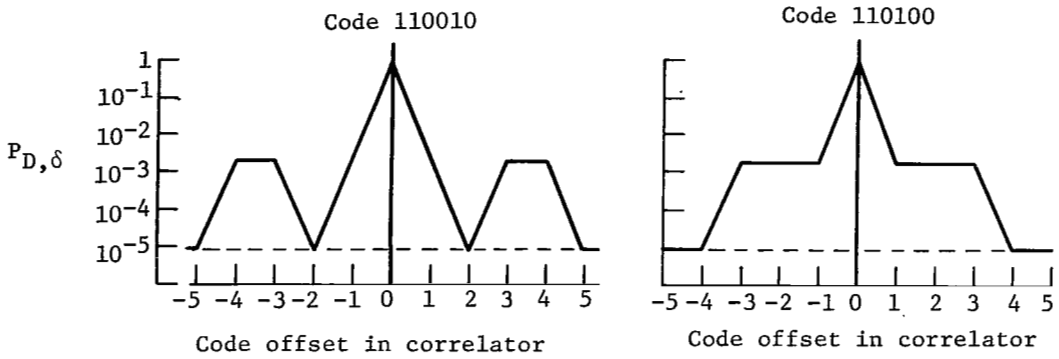

(a) Cross-correlation method 1.

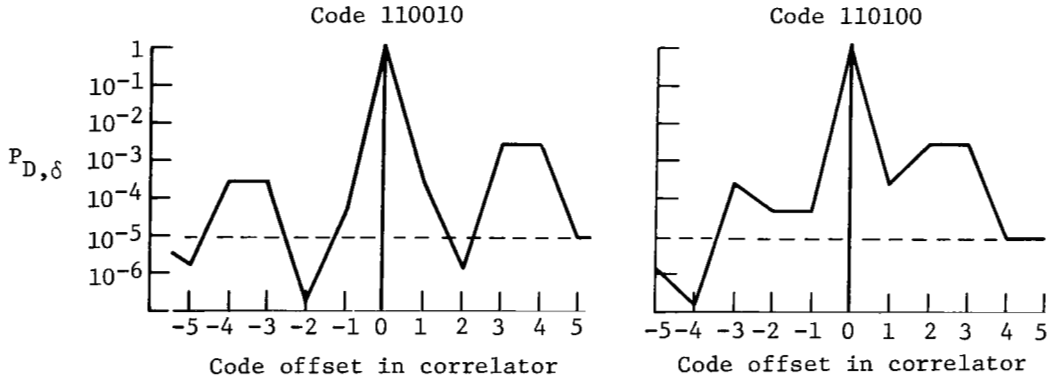

(b) Cross-correlation method 2.

Figure 9.- Probability-of-detection curves for example codes. The dashed line indicates the level of P_{FA} when no star code elements are in the correlator.

that the received code is perfectly detected and is preceded and followed by all 0's. For method 1 the total 1 bit agreements are plotted against code position, while for method 2 the total 1 plus 0 bit agreements are used. From a comparison of figures 9 and 10, it is evident that the corresponding curves have the same shapes. Hence, qualitative code comparisons could be made by comparing agreement levels and curve spreads such as those plotted in figure 10.

For the two codes studied, the probability of false detection is less with negative code offsets than with positive code offsets for method 2. For those cases, if two or more detections occur during one entire code correlation process, the first detection should be chosen as the star position. It is important to note that although method 1 cross correlation detects only 1's, the arrangement of 1's and 0's still affects the probability-of-detection curves, as shown in figure 9.

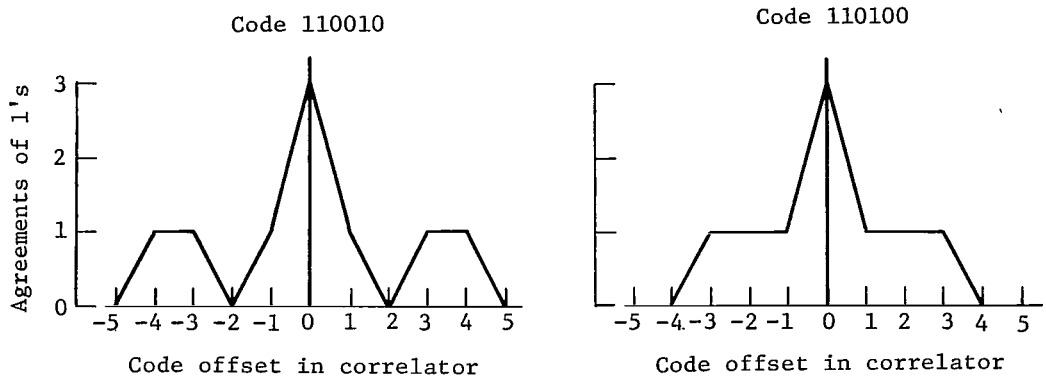

(a) Cross-correlation method 1.

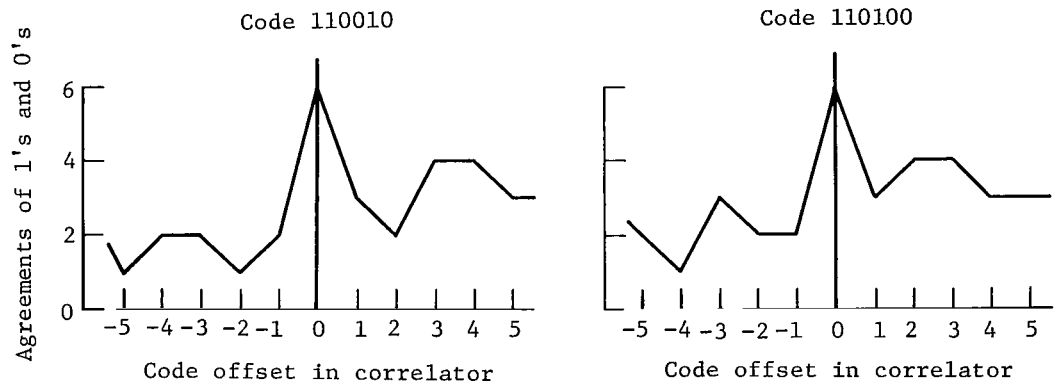

(b) Cross-correlation method 2.

Figure 10.- Agreement-level curves for example codes.

Synchronization Limitations

Although in the theoretical analysis it is assumed that synchronization is known, in the actual system it is impossible to know when to expect a star pulse. However, it is possible to know the repetition rate within limited accuracy. This can be calculated from the vehicle spin rate ω, which is obtained by any suitable means. The photomultiplier output can be sampled several times faster than the calculated bit rate so that a sufficient number of integrated samples are obtained within the star pulse width time t_B. It is desirable to know how much faster than the repetition rate the sampling rate must be, within what accuracy the repetition rate must be known, and what effect these factors have on the original theoretical prediction.

Let the following describe a typical code pattern:

f_r repetition bit rate of actual code to be sampled

sf_r ideal repetition rate of sampling process

νsf_r actual repetition rate of sampling process where ν is the error factor

2N total number of bits in the code

Let the original synchronized code to be sampled be represented by a square wave as shown in figure 11(b). For $s = 5$, figure 11(c) shows the results of a perfectly sampled code, that is, both f_r and synchronization are known. Figure 11(d) shows three possible unsynchronized cases, with uncertain samples indicated by hatching. If synchronization is not known but f_r is, then it is possible that as many as one sample out of every five will not have been taken accurately. This condition is independent of code length since f_r is known, and in general (s - 1) samples per original code bit can be utilized.

Allowing sf_r to lie in error will make the sampling process occur too fast or too slow according to the error factor ν. If every sth (every 5th in fig. 11) sample is compared with the bits of the known code, then there is a maximum and minimum ν for which a proper correlation will occur for at least one of the sets of every sth sample. Figure 11(e) shows this situation where the first good sample of each bit is the one to be correlated. As many as three samples at the end of the sampled code could be in error and still permit a proper correlation. Such a situation would occur when $\nu f_r < f_r$. Similarly, figure 11(f) utilizes the last good sample of each bit. Again as many as three samples at the end of the sampled code could be in error. This situation would occur when $\nu f_r > f_r$. Since the sampled bits are shifted through the correlator in a serial manner, bit-by-bit fashion, both correlation situations described above will occur during each five correlation processes. Therefore, the proper correlation is guaranteed if the error is kept within the allowed limits, which are $\pm \frac{s - 2}{s}\left(\frac{1}{f_r}\right)$ seconds for a code 2N bits long.

The desired error limitation can now be calculated. From the previous discussion the limits of ν can be expressed as

$$\frac{1}{t_s + \Delta t} \leqq \nu sf_r \leqq \frac{1}{t_s - \Delta t}$$

$$\frac{1}{sf_r\left(\frac{1}{sf_r} + \frac{s - 2}{sf_r 2Ns}\right)} \leqq \nu \leqq \frac{1}{sf_r\left(\frac{1}{sf_r} - \frac{s - 2}{sf_r 2Ns}\right)}$$

$$\frac{1}{1 + \frac{s - 2}{2Ns}} \leqq \nu \leqq \frac{1}{1 - \frac{s - 2}{2Ns}}$$

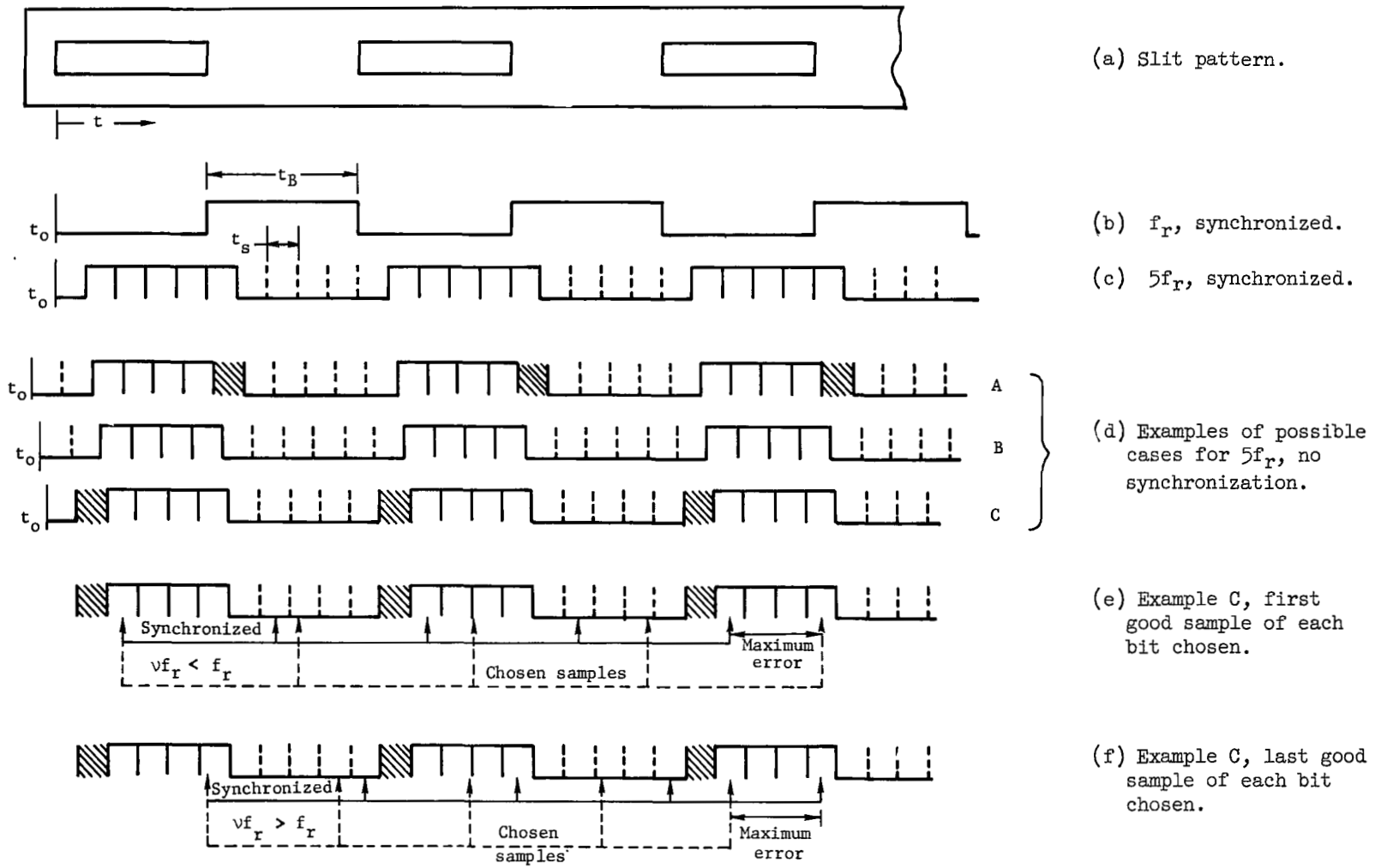

(a) Slit pattern.

(b) f_r, synchronized.

(c) $5f_r$, synchronized.

(d) Examples of possible cases for $5f_r$, no synchronization.

(e) Example C, first good sample of each bit chosen.

(f) Example C, last good sample of each bit chosen.

Figure 11.- Sampled code pattern.

$$\nu_{min} = \frac{1}{1 + \frac{s - 2}{2Ns}} \qquad \nu_{max} = \frac{1}{1 - \frac{s - 2}{2Ns}} \tag{22}$$

where

s integral multiple of exact code repetition rate

t_s sample length in time

Δt uncertainty in sample time

If ν_{min} of relations (22) is set equal to 1, then $s = 2$. Thus a sampling rate of at least twice the code repetition rate is required even if f_r is perfectly known. In figure 12 ν_{min} is shown as a function of sampling rate s for various code lengths. It is readily seen that for a given s, ν_{min} approaches 1 as N increases (the error permitted in the sampling rate measurement decreases). Thus for a given accuracy limitation a maximum usable code is established.

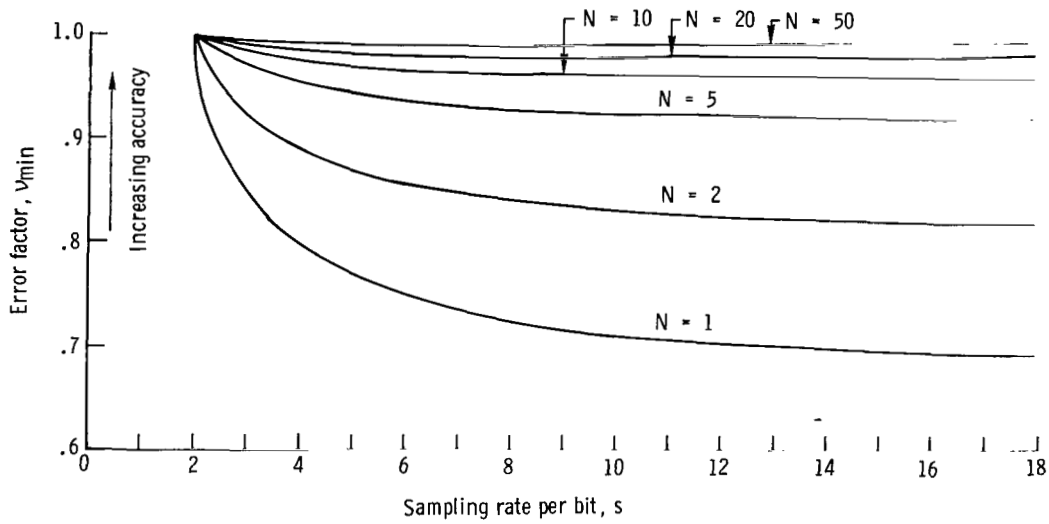

Figure 12.- Error factor as a function of sampling rate per bit for various code lengths 2N.

Unfortunately, the synchronization limitations have not only affected the maximum allowable code length, but also degraded the probability of detection. The integration time has been divided by s. In other words, now $\tau = \frac{t_B}{s}$ and $\lambda = \frac{k_n t_B}{s}$ (from eq. (2)). It should be recalled that the conclusion from the theoretical analysis was that decreasing λ decreased the probability of detection.

Photomultiplier Tube Noise

Dark current.- Spontaneous emission of electrons (those that occur when the photodetector is completely shielded from external radiation) within the photomultiplier constitutes the source of dark current (ref. 7). Since the detection statistics used the parameter of photoelectrons per sample (eq. (2)), the effect of dark current should be analyzed by using an equivalent dark-current photoelectron rate. This is

$$\overline{D} = \frac{\bar{I}_D t_s}{e\overline{G}} \tag{23}$$

where

$\overline{D}$ equivalent average dark-current rate, photoelectrons per sample

$\bar{I}_D$ average anode dark current, amperes

e electron charge, coulombs

$\overline{G}$ average multiplier gain

Dark current is not a function of the number of slits N, but is a function of the tube design, operating voltages, and environment. Thus dark current is included in the theoretical analysis by adding $\overline{D}$ to each noise term of equation (2). Obviously it has the same effect as background light (although it is not a function of N) and will decrease the probability of detection.

Secondary emission noise.- The use of a discrete photoelectron counter as a detector was implicit in the assumption that the electron multiplier gain was the same for each photoelectron. Thus, there was no difference between counting photoelectrons at the cathode and counting bundles of electrons at the anode. In reality such an assumption is not valid.

Much of the early work with electron multipliers involved investigations of the variation of gain due to the statistics of the secondary emission process. These studies resulted in the conclusion that the noise was a function of several parameters, including the emitter surface and the total number of dynodes (ref. 8). It was also shown that the use of the Poisson distribution to describe the gain of each dynode did not account for all the additional noise (ref. 9).

The total variance may be written as

$$\sigma_T^2 = k\tau \frac{\overline{\gamma}}{\overline{\gamma} - 1} b = k\tau(1 + B) \tag{24}$$

where

$k\tau$ variance of conventional shot noise (eq. (1))

$\bar{\gamma}$ average gain per dynode

b additional noise factor

$$1 + B = \frac{\bar{\gamma}}{\bar{\gamma} - 1} b$$

The term $\frac{\bar{\gamma}}{\bar{\gamma} - 1}$ was theoretically derived by Morton on the assumption that Poisson statistics applied to secondary emission (ref. 10). Since this is not adequate, as described above, the term b was included to make the equality valid. Winans and Pierce used the term $1 + B$ and from laboratory data believed that it usually lies between 1.5 and 3.0. They noted that $1 + B$ can be determined only by experiment (ref. 8).

Obviously the additional variance will degrade the system performance. For a given false-alarm probability, the result will be a significant reduction of the probability of detection.

The effect of limited synchronization knowledge and of photomultiplier noise can be included in the statistical analysis through use of the following equations:

Noise variance,

$$\left(\frac{N\lambda}{s} + \bar{D}\right)(1 + B) \tag{25a}$$

Signal variance,

$$\frac{\Gamma\lambda}{s}(1 + B) \tag{25b}$$

Signal and noise variance,

$$\left[\frac{\lambda}{s}(N + \Gamma) + \bar{D}\right](1 + B) \tag{25c}$$

CONCLUDING REMARKS

An investigation was made to determine the optimum detection scheme for a star-field mapping system that uses coded detection resulting from starlight shining through

specially arranged multiple slits of a reticle. It was determined that an optimum scheme should be based on the Neyman-Pearson criterion (fixed false-alarm probability) rather than the Bayes criterion. With threshold levels established by the Neyman-Pearson criterion, computer solutions of equations derived from the simplified theory showed that the probability of detecting a star could not be improved by using multiple slits in the modulating reticle. However, interpretation of the data showed that the use of multiple slits improved the system's ability to reject undesirable lower intensity stars. The number of slits for optimum rejection is not explicit, since it involves a trade off between the probability of detection desired for the stars to be rejected and the minimum allowable probability of detection for the lower intensity stars to be mapped.

A study of code construction showed that some codes are superior to others in terms of rms star-position error. It was demonstrated that method 2 (both 0 and 1 correlation) offered better position error characteristics than method 1 (only 1 correlation) for the cases analyzed. Since analysis showed that method 2 was also superior in rejection properties, it can be said that method 2 cross-correlation is superior to method 1 cross-correlation. Also, comparative results indicate that codes can be studied qualitatively with a simple technique of plotting the 1 and 0 agreements for various code offsets.

Analysis of the synchronization problem showed that it was possible to sample at a multiple of the expected repetition rate even if the rate was not known perfectly. The repetition rate error was shown to determine the necessary sampling rate and the maximum code length that could be utilized. The effect of multiple sampling was to decrease the resulting probability of detection.

Equations that were used for the simplified theoretical analysis were modified to take into account photomultiplier-tube dark-current and secondary-emission noise. The use of these equations in a new analysis, with experimentally determined values for the noise parameters, would result in lower probabilities of detection.

Langley Research Center,
National Aeronautics and Space Administration,
Hampton, Va., June 25, 1970.

APPENDIX

JUSTIFICATION FOR COUNTING PHOTOELECTRONS

The purpose of this appendix is to justify the simplification of the detection process to that of counting photoelectrons. The following definitions apply for this appendix only:

A	effective area of optics
c	speed of light
$E(\lambda)$	energy, joules per photon
$H(\lambda)$	transmission of optics as a function of λ
h	Planck's constant
$\overline{P}$	total average power
$\overline{P}_\lambda$	average power spectral density
$\overline{p}$	average number of photoelectrons per second
R_λ	spectral radiance of a star
$\overline{r}(\lambda)$	average number of photons per second
$\overline{\delta}(\lambda)$	average quantum efficiency of photocathode as a function of λ
λ	wavelength

The energy associated with one photon is

$$E(\lambda) = \frac{hc}{\lambda} \tag{A1}$$

Thus the average arrival rate of photons is related to the average power by

$$\overline{r}(\lambda) = \frac{\overline{P}}{E(\lambda)} = \frac{\overline{P}_\lambda}{hc} \tag{A2}$$

Since the spectral radiance of a star is expressed as an average power spectral density, the average number of photoelectrons per second for a given $d\lambda$ becomes

$$d\bar{p} = \frac{\left(\bar{P}_\lambda \, d\lambda\right)}{hc} \tag{A3}$$

where

$$\bar{P}_\lambda = R_\lambda A H(\lambda) \bar{\delta}(\lambda) \tag{A4}$$

The total average number of photoelectrons emitted from the photocathode is

$$\bar{p} = \int^{\lambda} d\bar{p} = \frac{A}{hc} \int_0^{\infty} R_\lambda H(\lambda) \bar{\delta}(\lambda) d\lambda \tag{A5}$$

where $\bar{p} \rightarrow k$ in the theoretical analysis (eq. (1)).

Note that although $\bar{\delta}(\lambda)$ represents an average quantum efficiency at a given λ, the use of Poisson statistics is not altered. This was shown by Steinberg and LaTourette (ref. 11).

REFERENCES

1. Walsh, T. M.; and Kenimer, Robert L.: Analysis of a Star-Field Mapping Technique for Use in Determining the Attitude of a Spin-Stabilized Spacecraft. NASA TN D-4637, 1968.

2. Feller, William: An Introduction to Probability Theory and Its Applications. Vol. I. John Wiley & Sons, Inc., c.1950.

3. Solodovnikov, V. V.: Introduction to the Statistical Dynamics of Automatic Control Systems. Dover Publ., Inc., 1937.

4. Spiegel, Murray R.: Theory and Problems of Statistics. McGraw-Hill Book Co., Inc., c.1961.

5. Harman, Willis W.: Principles of the Statistical Theory of Communication. McGraw-Hill Book Co., Inc., c.1963.

6. Williard, Merwin W.: Optimum Code Patterns for PCM Synchronization. Paper 5-5 of Proceedings of the 1962 National Telemetering Conference, vol. 1, May 1962. (Sponsored by ARS, AIEE, IAS, ISA, and IRE.)

7. Spicer, W. E.; and Wooten, F.: Photoemission and Photomultipliers. Proc. IEEE, vol. 51, no. 8, Aug. 1963, pp. 1119-1126.

8. Winans, R. C.; and Pierce, J. R.: Operation of Electrostatic Photo-Multipliers. Rev. Sci. Instrum., vol. 12, no. 5, May 1941, pp. 269-277.

9. Shockley, W.; and Pierce, J. R.: A Theory of Noise for Electron Multipliers. Proc. IRE, vol. 26, no. 3, March 1938, pp. 321-332.

10. Morton, G. A.: The Scintillation Counter. Vol. IV of Advances in Electronics, L. Marton, ed., Academic Press, Inc., 1952, pp. 69-107.

11. Steinberg, H. A.; and LaTourette, J. T.: A Note on Photon-Electron Converters With Reference to a Paper by A. Arcese. Appl. Opt., vol. 3, no. 7, July 1964, p. 902.

NASA-Langley, 1970 —— 14 L-6477

"The aeronautical and space activities of the United States shall be conducted so as to contribute . . . to the expansion of human knowledge of phenomena in the atmosphere and space. The Administration shall provide for the widest practicable and appropriate dissemination of information concerning its activities and the results thereof."

—NATIONAL AERONAUTICS AND SPACE ACT OF 1958

NASA SCIENTIFIC AND TECHNICAL PUBLICATIONS

TECHNICAL REPORTS: Scientific and technical information considered important, complete, and a lasting contribution to existing knowledge.

TECHNICAL NOTES: Information less broad in scope but nevertheless of importance as a contribution to existing knowledge.

TECHNICAL MEMORANDUMS: Information receiving limited distribution because of preliminary data, security classification, or other reasons.

CONTRACTOR REPORTS: Scientific and technical information generated under a NASA contract or grant and considered an important contribution to existing knowledge.

TECHNICAL TRANSLATIONS: Information published in a foreign language considered to merit NASA distribution in English.

SPECIAL PUBLICATIONS: Information derived from or of value to NASA activities. Publications include conference proceedings, monographs, data compilations, handbooks, sourcebooks, and special bibliographies.

TECHNOLOGY UTILIZATION PUBLICATIONS: Information on technology used by NASA that may be of particular interest in commercial and other non-aerospace applications. Publications include Tech Briefs, Technology Utilization Reports and Notes, and Technology Surveys.

Details on the availability of these publications may be obtained from:

SCIENTIFIC AND TECHNICAL INFORMATION DIVISION

NATIONAL AERONAUTICS AND SPACE ADMINISTRATION

Washington, D.C. 20546